REPORT DOCUMENTATION PAGE

Form Approved
OMB No. 0704-0188

1. REPORT DATE *(DD-MM-YYYY)*	**2. REPORT TYPE**	**3. DATES COVERED** *(From - To)*
Nov-2011	Technical Paper	November 2011-January 2012

4. TITLE AND SUBTITLE
Large Eddy Simulation of Flame-Turbulence Interactions in a LOX/CH4 Shear Coaxial Injector

5a. CONTRACT NUMBER
FA9300-10-C-0010

5b. GRANT NUMBER

5c. PROGRAM ELEMENT NUMBER

6. AUTHOR(S)

Masquelet, Guezennec, and Menon

5d. PROJECT NUMBER

5e. TASK NUMBER

5f. WORK UNIT NUMBER
33SP07KR

7. PERFORMING ORGANIZATION NAME(S) AND ADDRESS(ES)

Air Force Research Laboratory (AFMC)
AFRL/RQRC
10 E. Saturn Blvd.
Edwards AFB CA 93524-7680

8. PERFORMING ORGANIZATION REPORT NO.

9. SPONSORING / MONITORING AGENCY NAME(S) AND ADDRESS(ES)
Air Force Research Laboratory (AFMC)
AFRL/RQR
5 Pollux Drive
Edwards AFB CA 93524-7048

10. SPONSOR/MONITOR'S ACRONYM(S)

11. SPONSOR/MONITOR'S REPORT NUMBER(S)
AFRL-RZ-ED-TP-2012-100

12. DISTRIBUTION / AVAILABILITY STATEMENT
Distribution A: Approved for Public Release; Distribution Unlimited. PA#12245

13. SUPPLEMENTARY NOTES
Conference paper for the 50th AIAA Aerospace Sciences Meeting Including the New Horizons Forum and Aerospace Exposition, Nashville, Tennessee 9-12 January 2012.

14. ABSTRACT

This paper deals with the Large-Eddy Simulation of a cryogenic flame issued from a LOX-CH4 shear coaxial injector. The operating pressure is above the critical pressure for both propellants but oxygen is injected below its critical temperature. Such a state is referred to as transcritical and is representative of the extreme conditions which prevail in liquid rocket engines. Transcritical flows also exhibits large variations of density and strong departure from the perfect gas behaviour. To handle this problem, the solver uses a hybrid upwind-central scheme able to capture the sharp density gradients and the real gas thermodynamics is modeled using a cubic equation of state. Finite-rate chemistry is modeled using a modified one step CH4/air mechanism. Then, the filtered reaction rate for each species is closed by correcting the resolved reaction rate with a subgrid turbulent contribution. Two simple forms of this closure have been tested and compared. Qualitative comparisons with experimental data show that the LES is able to capture the turbulent structure of the flame. A dominant diffusion mode of combustion is reported and the flame is observed to be attached to the LOX post.

15. SUBJECT TERMS

16. SECURITY CLASSIFICATION OF:			**17. LIMITATION OF ABSTRACT**	**18. NUMBER OF PAGES**	**19a. NAME OF RESPONSIBLE PERSON**
					Doug Talley
a. REPORT	**b. ABSTRACT**	**c. THIS PAGE**			**19b. TELEPHONE NO** *(include area code)*
Unclassified	**Unclassified**	**Unclassified**	SAR	18	661-275-6174

50th AIAA Aerospace Sciences Meeting including the New Horizons Forum and Aerospace Exposition
09 - 12 January 2012, Nashville, Tennessee

AIAA 2012-1267

Large Eddy Simulation of Flame-Turbulence Interactions in a LOX-CH_4 Shear Coaxial Injector

Nicolas Guézennec*, Matthieu Masquelet† and Suresh Menon‡
Georgia Institute of Technology, Atlanta, GA, 30332-0150, USA

This paper deals with the Large-Eddy Simulation of a cryogenic flame issued from a LOX-CH4 shear coaxial injector. The operating pressure is above the critical pressure for both propellants but oxygen is injected below its critical temperature. Such a state is referred to as transcritical and is representative of the extreme conditions which prevail in liquid rocket engines. Transcritical flows also exhibits large variations of density and strong departure from the perfect gas behaviour. To handle this problem, the solver uses a hybrid upwind-central scheme able to capture the sharp density gradients and the real gas thermodynamics is modeled using a cubic equation of state. Finite-rate chemistry is modeled using a modified one step CH4/air mechanism. Then, the filtered reaction rate for each species is closed by correcting the resolved reaction rate with a subgrid turbulent contribution. Two simple forms of this closure have been tested and compared. Qualitative comparisons with experimental data show that the LES is able to capture the turbulent structure of the flame. A dominant diffusion mode of combustion is reported and the flame is observed to be attached to the LOX post.

I. Introduction

Large Eddy Simulation (LES) is becoming a standard tool to study turbulent combustion. The application of this method to model flames in liquid rocket engines remains however a challenging task. The difficulty of such a simulations is mainly due the transcritical conditions which usually prevail in the system: propellants are injected at cryogenic temperature below the critical temperature ($T < T_c$) while pressure exceeds the critical value ($P > P_c$). Under this regime, surface tension and latent heat become null.[1] Atomization and vaporization are replaced by continuous mixing processes dominated by diffusion and turbulent convection.[2–4] Moreover gas and liquid can not be distinguished: transcritical fluids may be very dense while keeping gas like-properties.[5]

During the last two decades, several experimental studies have been carried out on cryogenic flames[6–9] and they have shown important differences between subcritical and supercritical combustion. At subcritical pressure, the competition between dynamic forces and surface tension entails the liquid core break-up and generates a spray. Then atomization is followed by vaporization and combustion. For this regime, the flame stabilization mechanism depends of the fuel (CH4 or H2) and of the injection conditions. The flame may be lifted in the Oxidizer/Fuel shear layer or it may be anchored at the LOX post.[9] Above the supercritical pressure, droplets are replaced by small finger-like structures which dissolve in the light medium surrounding the transcritical jet.[7] Under these conditions, the flame attachment on the injector tip is systematically observed.

Substantial progress have also been obtained in the modeling and the simulation of transcritical combustion. Harstad et al.[10] proposed a computationally efficient method based on the departure function

*nicolas.guezennec@ae.gatech.edu, Research Scientist, Computational Combustion Laboratory, School of Aerospace Engineering.
†gtg540e@mail.gatech.edu, Graduate Research Assistant, Computational Combustion Laboratory, School of Aerospace Engineering, and AIAA Student Member.
‡suresh.menon@gatech.edu, Professor, Director of Computational Combustion Laboratory, School of Aerospace Engineering, and Associate Fellow AIAA.

and the Peng-Robinson Equation of state to describe thermodynamic properties of fuel/oxidant mixtures. This method has been widely applied in CFD and has shown good accuracy. Large Eddy Simulation and Direct numerical simulations, mainly carried out on mixing layers and coaxial configurations for LOX/H2 flames,[4,11,12] have extended the understanding of the processes which control transcritical combustion. By computing a sector of the single element experiment of Oschwald et al,[7] Oefelein[13] was able to provide a detailed characterization of the LOX/H2 flame near field. He also identified the primary holding mechanism leading to the flame attachment on the injector tip.

This paper proposes a LES strategy to solve transcritical oxy-combustion of methane. The choice of methane is driven by the recent interest for this fuel as an alternative to hydrogen. Even if it has not been widely utilized for spacecraft applications, many arguments suggest that the next generations of rockets will include engines operating with cryogenic methane. Its diffusivity is lower and its liquefaction temperature is higher than hydrogen. This would allow to design lighter tanks and by extension might increase the pay load of the future space vehicles.

The combustion of methane at high pressure also raises new questions and new challenges. First, the density and the critical temperature of this gas are high compared to hydrogen. This allows a large range of injection condition and by extension a large range of combustion regimes that CFD tools must be able to handle. The experiment carried out on a shear coaxial injector by Singla et al.[14] illustrates this point. They have shown that when methane and oxygen are both injected below the critical temperature, the flame exhibits a large expansion angle. Moreover, combustion takes place in two distinct regions: in the inner and the outer shear layers of the coaxial jet. The same experience repeated with supercritical methane provides one zone of combustion in the shear layer between the oxygen and the fuel streams and a smaller angle of expansion is observed. Finally, if detailed mechanisms can be now applied to model finite rate chemistry in LES of hydrogen-oxygen flames,[15] their equivalents for methane remain too expensive to be utilized with high fidelity simulation technics. For comparison, the detailed high pressure hydrogen-oxygen mechanism proposed by Conaire et al[16] consists of 21 elementary steps among 8 species while the GRI-Mech 3.0[17] mechanism contains 325 steps and 53 species. This issue adds complexity to the open question of the the reaction rate closure. The flamelet approach[18] which assumes an infinitely fast chemistry is a quite inexpensive method which can circumvents this problem. But for many rocket applications where the flame may experience high strain rate an local extinction, this method becomes inappropriate since the chemical time scales and the flow time scales may be comparable. Finite rate chemistry closures such as the Linear Eddy Model (LEM)[19] would be more suitable to simulate this kind of configuration.

In the present study, a Large Eddy Simulation of the LOX/CH4 Mascotte test rig (Version 4)[14] has been carried out for the operating point G2. Recent numerical studies of this case using RANS[20] and LES[21] with infinitely fast combustion models have provided a good representation of the experimental flame and have shown strong real gas effects on its structure. This paper first presents the formulation applied to model the LES equations, the thermodynamics and the transport properties. A simple LES finite rate chemistry approach is also proposed to close the combustion reaction rate. Then, the experimental configuration and the numerical setup are detailed. Finally, the calculation of the transcritical flame is discussed and qualitatively compared with the experiment.

II. Formulation

II.A. LES closure

The current solver deals with a Favré-filtered version of the compressible, multi-species and unsteady Navier-Stokes equations in conservative form. Following Erlebacher et al.,[22] the flow variables are decomposed by a spatial filtering operation (denoted by an overbar $\overline{f}$) and two separate fields are obtained: the unresolved, or sub-grid, scale and the resolved, or super-grid, scale represented by a tilde ($\tilde{f} = \frac{\overline{\rho f}}{\overline{\rho}}$). The filtered equations, respectively for mass conservation (1), momentum conservation (2), energy conservation (3) and species conservation (4), read:

$$\frac{\partial \overline{\rho}}{\partial t} + \frac{\partial \overline{\rho}\widetilde{u}_i}{\partial x_i} = 0 \tag{1}$$

$$\frac{\partial \overline{\rho}\widetilde{u}_i}{\partial t} + \frac{\partial}{\partial x_j}\left(\overline{\rho}\widetilde{u}_i\widetilde{u}_j + \overline{p}\delta_{ij} - \overline{\tau}_{ij} + \tau_{ij}^{\mathrm{sgs}}\right) = 0 \tag{2}$$

$$\frac{\partial \overline{\rho}\widetilde{e_T}}{\partial t} + \frac{\partial}{\partial x_i}\left(\overline{\rho}\widetilde{e_T}\widetilde{u_i} + \overline{p}\widetilde{u_i} + \overline{Q}_{i,\mathrm{IK}} - \widetilde{u}_j\overline{\tau}_{ji} + H_i^{\mathrm{sgs}} + \sigma_i^{\mathrm{sgs}}\right) = 0 \tag{3}$$

$$\frac{\partial \overline{\rho}\widetilde{Y}_k}{\partial t} + \frac{\partial}{\partial x_i}\left(\overline{\rho}\widetilde{Y}_k\widetilde{u}_i + \overline{J}_{i,k} + Y_{i,k}^{\mathrm{sgs}} + \theta_{i,k}^{\mathrm{sgs}}\right) = \overline{\dot{\omega}}_k \;\text{ for }\; k = 1\cdots N_S \tag{4}$$

The closure of the system above is an issue. $N_S + 5$ equations have been written to obtain the $N_S + 5$ conservative variables,but several other quantities have been introduced: the filtered pressure $\overline{p}$, the heat flux $\overline{Q}_{i,\mathrm{IK}}$ (in its "Irving-Kirkwood" form including the enthalpy flux by mass diffusion), the mass flux $\overline{J}_{i,k}$ and several sub-grid terms (τ_{ij}^{sgs}, H_i^{sgs}, σ_i^{sgs}, $Y_{i,k}^{\mathrm{sgs}}$ and $\theta_{i,k}^{\mathrm{sgs}}$). The subgrid heat flux σ_i^{sgs} and the subgrid species diffusive flux $\theta_{i,k}^{sgs}$ are usually neglected because they have been shown to have a small magnitude at high Reynolds number.[23,24]

The mass and heat diffusion fluxes are solely based on Fick's and Fourier's types of diffusion:

$$\overline{Q}_{i,\mathrm{IK}} = -\overline{\lambda}\frac{\partial \widetilde{T}}{\partial x_i} + \overline{\rho}\sum_{k=1}^{N_S}\widetilde{h}_k\widetilde{Y}_k\widetilde{\mathcal{V}}_{i,k} + \sum_{k=1}^{N_S}Q_{i,k}^{\mathrm{sgs}} \tag{5}$$

$$\overline{J}_{i,k} = \overline{\rho}\widetilde{Y}_k\widetilde{\mathcal{V}_{i,k}} = -\overline{\rho}\overline{\mathcal{D}}_{k,m}\frac{\partial \widetilde{Y}_k}{\partial x_i} \tag{6}$$

with the approximation of evaluating the diffusion coefficient $\mathcal{D}_{k,m}$ of each species into the mixture instead of considering each individual binary diffusions. Thus the cross-diffusion Dufour and Soret terms are neglected in this study. Their significance under super-critical conditions is not always demonstrated[25] and their inclusion in a LES formulation would introduce additional unclosed terms that have not been studied yet.

Like σ_i^{sgs} and $\theta_{i,k}^{\mathrm{sgs}}$, the sub-grid enthalpy flux due to mass diffusion $Q_{i,k}^{\mathrm{sgs}}$ is neglected as a first approximation. The sub-grid enthalpy flux H_i^{sgs}, the sub-grid stress tensor τ_{ij}^{sgs} and the sub-grid species flux $Y_{i,k}^{\mathrm{sgs}}$ are closed using a gradient diffusion approach and a sub-grid eddy viscosity that uses the turbulent kinetic energy.[26]

The momentum closure will define the eddy viscosity. An additional transport equation is needed for this turbulent kinetic energy $k^{\mathrm{sgs}} = \frac{1}{2}\left(\widetilde{u_i u_i} - \widetilde{u}_i\widetilde{u}_i\right)$. Neglecting compressibility effects and assuming a simple gradient diffusion model for the sub-grid transport, this equation reads:

$$\frac{\partial \overline{\rho}k^{\mathrm{sgs}}}{\partial t} + \frac{\partial}{\partial x_i}\left(\overline{\rho}k^{\mathrm{sgs}}\widetilde{u}_i\right) = P^{\mathrm{sgs}} - \epsilon^{\mathrm{sgs}} - \overline{\rho}\frac{\nu_t}{\mathrm{Pr}_t}\frac{\partial k^{\mathrm{sgs}}}{\partial x_i} \tag{7}$$

The expressions for the production $P^{\mathrm{sgs}} = -\tau_{ij}^{\mathrm{sgs}}\frac{\partial \widetilde{u}_i}{\partial x_j}$ and dissipation $\epsilon^{\mathrm{sgs}} = C_\epsilon\overline{\rho}\frac{\sqrt{(k^{\mathrm{sgs}})^3}}{\overline{\Delta}}$ terms leave only two model coefficients, C_ν and C_ϵ to complete the sub-grid closure. In this study, C_ν and C_ϵ are constant, respectively equal to 0.067 and 0.916. These values were evaluated in earlier studies[27] without any *a priori* assumptions of ideal gas behavior but assuming incompressible flows. The turbulent Prandtl and Schmidt numbers are also assumed constant with, respectively, values of 0.9 and 0.7.

II.B. Thermodynamics and transport properties

Among the cubic equation of state listed by Poling et al.,[1] the Peng-Robinson equation of state is the one chosen for this study:

$$p = \frac{R_u T}{V_m - B} - \frac{A}{V_m^2 + 2V_m B - B^2} \tag{8}$$

where V_m is the molar volume, R_u is the universal gas constant. The first term $\frac{R_u T}{V_m - B}$ models the repulsive force that molecule exert on each other at short distance. The parameter B is proportional to the actual volume of the molecule. The second term $\frac{A}{V_m^2 + 2V_m B - B^2}$ models the long range attractive forces between the molecules such as electrostatic forces, polarization or London dispersion forces.

The transport properties are also affected by the transcritical conditions. It is required to apply robust models which are able to handle large variation of the fluid properties from a dense cryogenic fluid in the LOX flow to a light gas in the flame. For this study, a correction of the Chung model for high pressure has been applied: the viscosity μ and the thermal conductivity κ are computed using the Corresponding States

Method. The basic viscosity equation for a rigid non-attracting sphere[28] are solved, including the correction by Chung et al. for the shape and polarity.[29] The diffusion coefficients are modeled with a correction on the basic equation proposed by Fuller et al.[30]

II.C. Reduced Mechanism

If detailed mechanisms for CH4 combustion such as GRI-Mech 3.0 are now available, they involve too many species and reaction steps to be applicable in LES. Only a reduced mechanism with a few steps and species can be reasonably used for this type of simulation. However they are usually built for Air/CH4 flames and they match a small range of thermodynamic conditions (pressure, initial temperature...). For this study, CH4 has to burn with pure oxygen under high pressure. Therefore, correction of the one step mechanism of Westbrook and Dryer[31] is introduced here to predict adequate adiabatic flame temperature and flame speed under these conditions. The original mechanism is composed of $N_r = 1$ irreversible reaction involving $N_s = 4$ species CH4, O2, CO2, H2O:

$$CH_4 + 2O_2 \rightarrow CO_2 + 2H_2O \tag{9}$$

It will be called WD1 in the rest of the paper. Preliminary simulations of a CH4/O2 laminar premixed flame at $\varphi = 1$ with an initial temperature $T_0 = 300K$ were carried out using Cantera. The pressure was $P_0 = 5.6MPa$ which corresponds to the ambient pressure of the case G2 (See Table 2). The real gas equation of state was replaced by the perfect gas equation. The final composition in the burnt gas is easy to compute for WD1:

$$X_{CH_4} = X_{O_2} = 0, \;\; X_{CO_2} = \frac{\varphi}{\varphi + 2} = 1/3, \;\; X_{H_2O} = \frac{2\varphi}{\varphi + 2} = 2/3 \tag{10}$$

Moreover, the final adiabatic temperature T_{ad} is given by applying the first thermodynamic law to the system:

$$\sum_{i=1}^{4} (X_i - X^0{}_i)\Delta h^{0,m}_{f,i} + X_i \int_{T_0}^{T_{ad}} c^m{}_{p,i} dT - X^0_i \int_{T_{ref}}^{T_0} c^m{}_{p,i} dT = 0 \tag{11}$$

The resolution of Eq. (11) provides $T_{ad} = 5072K$. Table 1 compares the flame speed and the adiabatic flame obtained with WD1 and GRI-Mech 3.0. WD1 presents big discrepancies with the detailed kinetic chemistry which shows this mechanism is not adapted to oxycombustion.

A simple method to improve WD1 is presented here. The new reduced mechanism will be called WD1ox. First, The adiabatic temperature is overpredicted because the one step mechanism does not take account of dissociations. These reactions play an important role in oxycombustion. This problem can be solved by adding a term in the enthalpy equation (Eq. (11)) to model the chemical enthalpy of products which should occur during the reaction (CO, H ,H2...).

$$\Delta h^{0,m}_{f,dissociation} + \sum_{i=1}^{4} (X_i - X^0{}_i)\Delta h^{0,m}_{f,i} + X_i \int_{T_0}^{T_{ad}} c^m{}_{p,i} dT - X^0_i \int_{T_{ref}}^{T_0} c^m{}_{p,i} dT = 0 \tag{12}$$

$\Delta h^{0,m}_{f,dissociation}$ can also be expressed in function of the chemical enthalpy variation using a coefficient α_{diss}:

$$(1 - \alpha_{diss}) \sum_{i=1}^{4} (X_i - X^0{}_i)\Delta h^{0,m}_{f,i} + X_i \int_{T_0}^{T_{ad}} c^m{}_{p,i} dT - X^0_i \int_{T_{ref}}^{T_0} c^m{}_{p,i} dT = 0 \tag{13}$$

Eq. (13) can be solved using the adiabatic temperature predicted by GRI-Mech 3.0. It gives $\alpha_{diss} = 0.31$. In practice, the effect of dissociation can be added by multiplying the enthalpy of formation for each species by $1 - \alpha_{diss}$. In Cantera and LESLIE, thermochemistry is computed using the NASA polynomial interpolation:

$$H_i/RT = a_1 + a_2 T/2 + a_3 T^2/3 + a_4 T^3/4 + a_5 T^4/5 + a_6/T \tag{14}$$

According to Eq. 14, the enthalpy of formation for each species i is equal to a_6. In order to obtain the correct adiabatic temperature, this coefficient is multiplied by $1 - \alpha_{diss}$. The other quantities, $c^m{}_{p,i}$ and S_i are not affected by this modification since they don't depend of a_6.

Then the flame speed s_L must also be changed. The asymptotic analysis of Zeldovich, Frank-Kamenetski and Von Karman (ZFK)[32] demonstrates that s_L varies like the square root of the reaction rate coefficient A_f. Accordingly, a way to match the correct flame speed consist in modifying A_f:

$$A_{fcorrection} = A_f \left(\frac{s_{LGRI}}{s_{LWD1ox}} \right)^2 \tag{15}$$

where s_{LGRI} is the flame speed obtained with GRI-Mech 3.0 and s_{LWD1ox} is the flame speed given by WD1ox without any correction of A_f. The third line of Table 1 presents the adiabatic temperatures and the flame speed obtained with WD1ox. The corrected mechanism predicts these quantities with less than 5% error. However, WD1ox presents some limitations. Figure 1 shows that the agreement between WD1ox and GRI-Mech 3.0 is not perfect. The heat release maximal value is too high while it is underestimated for temperatures lower than 2000K. The ignition temperature is around 1500K whereas GRI-Mech 3.0 predicts combustion up to 750K. This issue can create extinctions when hot reactants are mixed with some colder gas by turbulent eddies.

	T_{ad} (K)	s_L (m/s)
GRI-Mech 3.0	3584	2.317
WD1	5051	11.11
WD1ox	3755	2.283

Table 1. Adiabatic temperature and flame speed obtained with Cantera

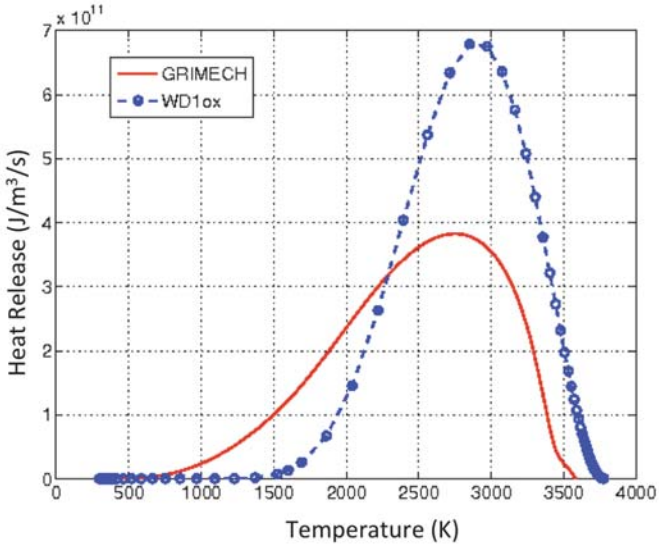

Figure 1. Premixed flame heat release versus temperature: comparison of WD1ox with GRI-Mech 3.0

II.D. LES Combustion Model

The last term to close in Eq. 4 is the LES filtered reaction rate $\overline{\dot{\omega}}_k$. The strategy chosen here consists in splitting $\overline{\dot{\omega}}_k$ between a large scale and a subgrid contribution:

$$\overline{\dot{\omega}}_k = F\dot{\omega}_k \left(\bar{\rho}, \widetilde{T}, \widetilde{Y}_i \right) + G\dot{\omega}_k^{sgs} \tag{16}$$

The large scale reaction rate $\dot{\omega}_k \left(\bar{\rho}, \widetilde{T}, \widetilde{Y}_i \right)$ is directly expressed from the Arrhenius laws of the chemical mechanism applied to the resolved field. The subgrid reaction rate $\dot{\omega}_k^{sgs}$ depends of the subgrid scale parameters, such as the subgrid kinetic energy, and must be modeled. The terms F and G are the blending functions which depend of the local flow conditions. Two simple forms of these functions have been tested:

LAM $F = 1$ and $G = 0$: the subgrid term is neglected. Mixing is assumed perfect at the subgrid level.

MAX $F = H(|\dot{\omega}_k| > |\dot{\omega}_k^{sgs}|)$ and $G = 1 - F$: where H is the Heaviside function. This model is equivalent to pick the maximum value between the laminar reaction rate and the subgrid reaction rate. The objective of this model is to replace the large scale reaction rate by the $\dot{\omega}_k^{sgs}$ only in the zones where the turbulent effects are high and where the flame can be diluted by cold gas which would entail the underestimation of the reaction rate by WD1ox and in some situations would generate extinctions. Therefore the model MAX forces combustion in locations where oxygen and methane are in contact but where the reaction rate predicted by the Arrhenius law is too low.

The procedure to compute the subgrid reaction rate is based on the Eddy Dissipation Combustion model (EDC). This approach is an evolution of the Eddy Break-Up model (EBU)[33,34] and was originally developed by Magnussen and Hjertager[35–37] for RANS. For each reaction, a subgrid mixing reaction rate is computed:

- If the reaction kinetics goes forward (formation of products) then the mixing is limited by the deficient reactant:

$$\dot{\omega}_j = -\frac{\bar{\rho}}{\tau_{sgs}} min\left(\frac{Y_k}{W_k \nu_{kj}^{reac}}\right) \tag{17}$$

- If the reaction kinetics goes backward (formation of reactants) then the mixing is limited by the deficient product:

$$\dot{\omega}_j = \frac{\bar{\rho}}{\tau_{sgs}} min\left(\frac{Y_k}{W_l \nu_{kj}^{prod}}\right) \tag{18}$$

where ν_{kj}^{prod} and ν_{kj}^{reac} are the stoichiometric coefficients and τ_{sgs} is the subgrid turbulent time scale which is estimated from the subgrid kinetic energy K_{sgs} and the cell volume V_{cell}:

$$\tau_{sgs} = \frac{V_{cell}^{1/3}}{\sqrt{K_{sgs}}} \tag{19}$$

Finally the subgrid reaction rate is expressed for each species k:

$$\dot{\omega}_k^{sgs} = W_k \sum_{j=1}^{nreac} \left(\nu_{kj}^{prod} - \nu_{kj}^{reac}\right) \dot{\omega}_j \tag{20}$$

This formulation is very similar to the LES subgrid model proposed by Fureby and Möller.[23] However the interpretation of $\dot{\omega}_k^{sgs}$ and $\dot{\omega}_k\left(\bar{\rho}, \widetilde{T}, \widetilde{Y_i}\right)$ is different. Fureby an Möller picked the minimum value of each contribution considering that the slowest phenomenon (mixing or chemistry) controls the reaction rate. This approach is consistent for RANS or coarse LES where a non negligible part of the turbulent mixing occurs at the subgrid scale. However for fine grids, it would asymptotically yields to a reaction rate equal to zero ($\tau_{sgs} = 0$). When most of the turbulent mixing scales are resolved by LES, the reaction rate is actually controlled by the chemistry: $|\dot{\omega}_k\left(\bar{\rho}, \widetilde{T}, \widetilde{Y_i}\right)| >> |\dot{\omega}_k^{sgs}|$. Therefore the decomposition of Eq. 16 is more accurate and converges to the correct DNS flame.

III. Experimental and numerical setup

III.A. The MASCOTTE V04 test case

This paper focuses on the simulation of the LOX/CH4 single-element shear coaxial injector investigated by Singla et al.[14] on the Mascotte test rig. This small scale thrust chamber is operated by ONERA. A detailed description of the experimental setup and of the instrumentation is given in previous papers.[14,38] The combustor is composed of a square chamber equipped with visualization windows on its four sides. The mean flame structure was obtained from Abel transform of OH and CH LIF emission images. Therefore only qualitative comparison between experiment and LES will be possible. Four operating points were studied, but only the case G2 at pressure above the critical point can be considered in this study. The flow conditions for this configuration are listed in Table 2. Methane is injected as a supercritical gas and the oxygen remains transcritical.

	$\dot{m}$ (g/s)	T (K)	P (MPa)	π_r
O2	44.4	85	5.61	1.11
CH4	143.1	288	5.61	1.24

Table 2. Experimental operating conditions for the case G2. The reduce pressure π_r designates the ratio between the operating pressure P and the critical pressure Pc

III.B. Numerical implementation

Even if surface tension and latent heat of vaporization vanish, transcritical flows still present very large density gradient due to mass and heat transfer from dense to light fluids.A previous study on LOX/H2 flames[39,40] have pointed the limitations of central scheme to predict such large density gradients and have shown the necessity of running a hybrid central-upwind scheme instead of a pure central scheme.

Consequently, the current fully compressible flow solver uses a finite-volume scheme with a second-order time-accurate predictor-corrector integration and a second-order accurate hybrid solver for spatial integration. This finite volume hybrid solver alternates between a second-order central scheme and a third-order accurate MUSCL, an upwind-biased scheme. A dynamic and local switch,[41] based on pressure and density gradients, determines (at each time step and computational face) which scheme to use. The MUSCL reconstruction technique is used alongside an approximate Riemann solver (specifically, Harten-Lax-Van Leer (HLL) from Génin and Menon,[42] with HLL contact/solver modifications by Toro et al.,[43] as well as the monotonized central limiter, to enforce the total variation diminishing condition. This hybrid scheme allows the capture of the large density gradients typically found near the injection plane while keeping the required grid resolution reasonable and keeping the less dissipative central scheme in the far field in order to accurately model the turbulence. Characteristic non-reflecting boundary conditions are employed at fuel and oxidizer inlets and at the computational domain outlet. No-slip adiabatic conditions are imposed at walls.

III.C. Computational grids

The computational domain is shown on Fig. 2a. It corresponds to the first 150 mm of the full experimental combustion chamber and includes the final part of the single shear coaxial injector. The reduction of the combustion is motivated by the very small length of the flame which is lower than 50 mm for all operating points. The length of the computational domain is sufficient to avoid any interaction between the reacting zone and the outlet. Finally, this operation enables to improve the resolution without increasing the computation cost. The simulations have been performed on a multiblock grid. The outer cylindrical block contains 765 x 233 x 129 grid points, while the inner butterfly Cartesian block contains 765 x 33 x 33 grid points (Fig. 2c) The finest resolution is located in the injector posttip region ($\Delta x = 30$ μm). The resolved kinetic energy spectrum in this region, shown in Figure 3, demonstrates the recovery of the Kolmogorov $-5/3$ spectrum, indicating sufficient resolution for a proper LES model.

IV. Results

This section discusses the results obtained for the two LES models described in section II.D. At this stage, only the LES of the model MAX has been completed. The laminar chemistry model LAM experienced strong extinction issues and could not be run enough to provide converged statistics. By default, most of the results presented in this papers will therefore refer to the subgrid closure MAX. Explicit references to LAM will be carried out when the two models are compared.

IV.A. Flame and flow Structure

To illustrate the turbulent flow structure, Figure 4a shows iso-contours of Q criterion colored with the velocity magnitude. The density isosurface $\rho = 150$ kg/s is also presented in purple to visualize the dense core. Annular coherent eddies occur in the shear layer between the methane stream and the quiescent environment. They entail gas from the low velocity zone to the high speed jet . These structures wrinkle the transcritical oxygen core and break down to generate a highly turbulent flow . The LES temperature

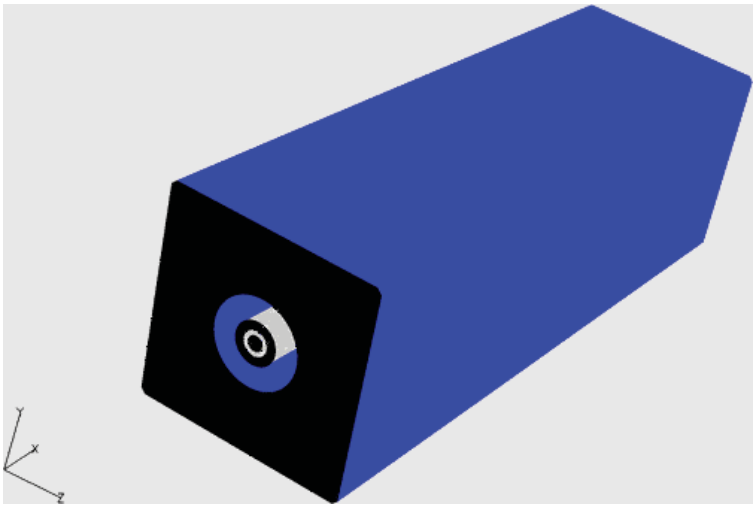

(a) Overall view

(b) Injector near-field

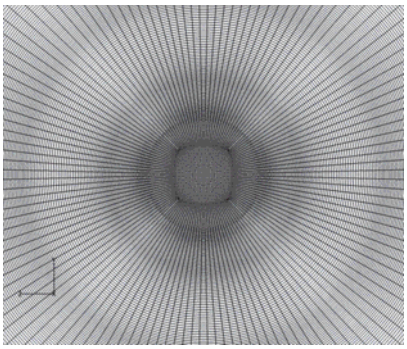

(c) Butterfly grid

Figure 2. Views of the grid for the Mascotte configuration

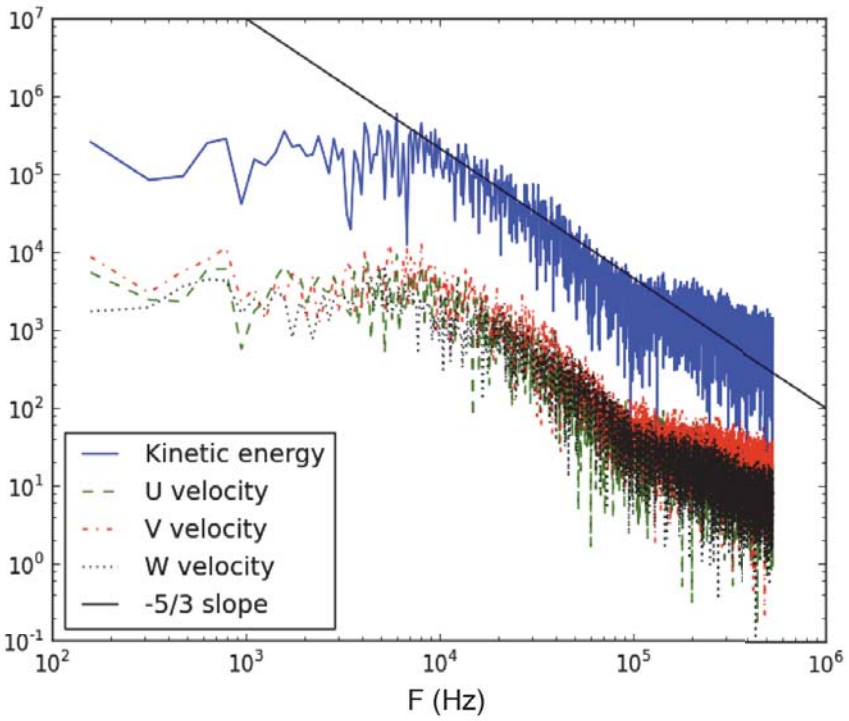

Figure 3. Resolved velocity and kinetic energy spectrum in the injector near field.

isosurface $T = 1700K$ is compared with a visualization of the experimental flame on Figure 4b. This qualitative comparison suggests a good agreement between LES and experiment. The flame is anchored on the tip between the CH4 and the LOX injection. The reaction zone is a short cone (around 6 cm) starting with an expansion angle lower than 10 ° and abruptly terminating with an angle of 20°.

Figure 5 presents the average (top) and the RMS (bottom) axial velocity field. The white line designates the temperature isocontour $\overline{T} = 1300$ K and helps to visualize the combustion zone. The flame strongly delays the transition from a coaxial jet to a single jet. Instead of converging towards the center line of the chamber, the methane stream is deflected towards the combustor walls owing to the gas expansion generated by the flame. A small zone of negative axial velocity is also visible in the vicinity of the LOX post. This wake plays an important role in the holding mechanism of the flame.[13] This creates recirculation of the hot products and stabilizes the flame by promoting the vaporization and the mixing of the dense LOX core.

This phenomenon is illustrated on Figures 6 and 7, which show instantaneous snapshots of the flow in the vicinity of the injector. For each subgrid model, a strong backflow of hot products anchors the flame on the tip wall. But some differences are noticeable. The laminar model presents a preferred flame stabilization on the oxidizer side of the injector while it is on the fuel side for the model MAX. But the direct anchoring of the flame is actually unphysical. OH-PLIF measurements carried out by Singla et al[38] have shown that the flame is lifted at a very short distance of the wall. Catching this phenomenon with LES is beyond the scope of our study. The adiabatic wall should be replaced by an isothermal boundary condition. This would also require a much finer resolution in the vicinity of the injector and a detailed mechanism able to predict low temperature kinetics.

IV.B. Combustion regime

Figure 8a presents scatter plots of species mass fraction (CH4, O2 and H2O) versus the mixture fraction z:

$$z = \frac{sY_{CH4} - Y_{O2} + Y^0_{O2}}{sY^0_{CH4} + Y^0_{O2}} \tag{21}$$

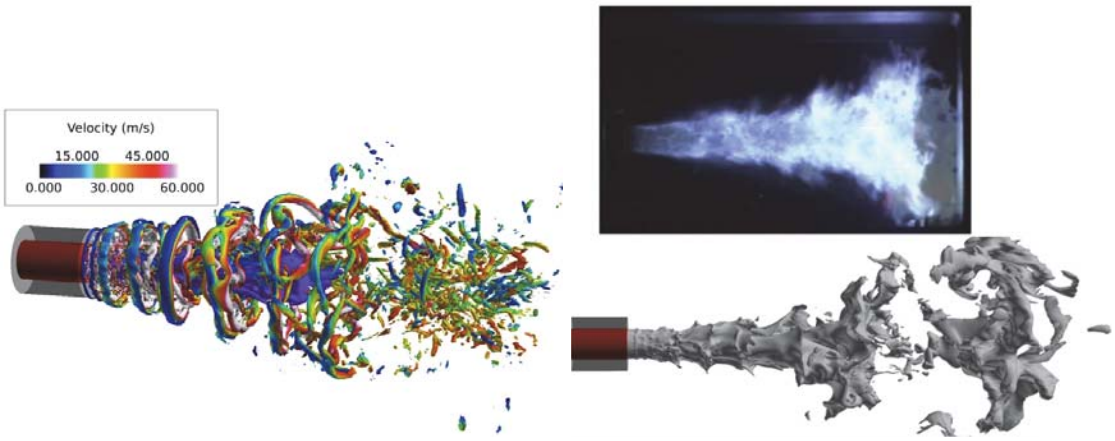

(a) (b)

Figure 4. Flame and flow structure: (a)Isosurfaces of Qcriterion (=5e8 s^-2) colored by the velocity magnitude and density isosurface $\rho = 150$ (purple). (b) top: visualization of the experimental flame,[14] bottom: LES temperature isosurface $T = 1700K$

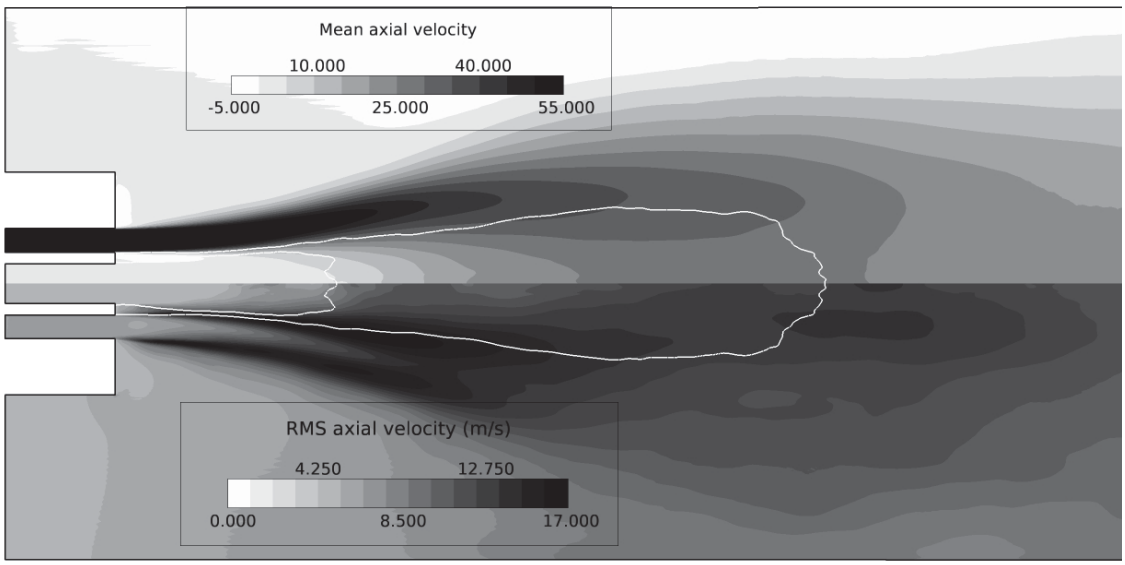

Figure 5. Average flow field: average axial velocity (top), RMS axial velocity (bottom). The white line corresponds to the mean temperature isocontour $\overline{T} = 1300$

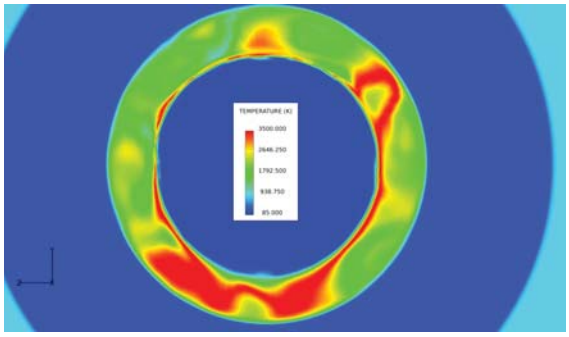

(a) XY plane: Temperature field on the sleeve wall

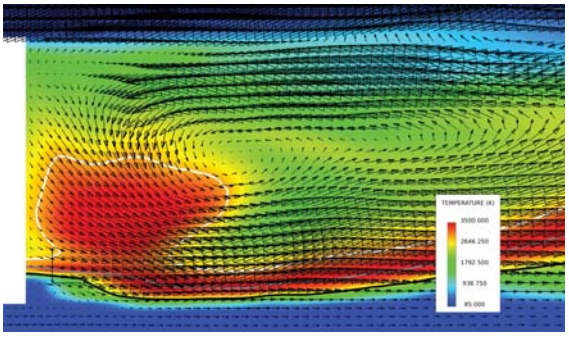

(b) YZ plane: Temperature and velocity fields in the vicinity of the tip wall. Isocontours of mixture fraction (black $z = 0.1$, grey $z = 0.2$, black $z = 0.3$)

Figure 6. Flame holding mechanism for the laminar chemistry model LAM.

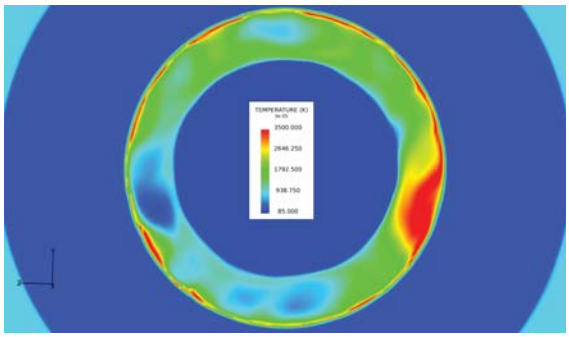

(a) XY plane: Temperature field on the sleeve wall

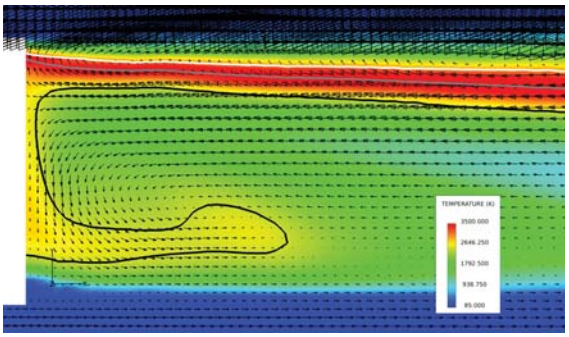

(b) YZ plane: Temperature and velocity fields in the vicinity of the tip wall. Isocontours of mixture fraction (black $z = 0.1$, grey $z = 0.2$, black $z = 0.3$)

Figure 7. Flame holding mechanism for the LES model MAX

where $s = 4$ is the stoichiometric mass ratio and $Y^0_{CH4} = Y^0_{O2} = 1$. The points gather around straight lines intersecting at the stoichiometric mixture fraction, $z = 0.2$, which suggests that an infinitely fast chemistry flamelet model is valid for the case G2. The diffusion regime is confirmed by the flame criterion[44] on Figure 8b. This quantity is defined as:

$$\Gamma_f = \nabla Y_{O_2} . \nabla Y_{CH4} \tag{22}$$

Negative values of Γ_f correspond to a diffusion flame and positive values define zones of partially-premixed combustion. The criterion shows very high negative values along the stoichiometric mixture fraction while nearly no positive value is observed elsewhere in the flame. This kind of situation is specific of the G2 case and is not really representative of the usual rocket operating conditions. The Reynolds number in real rocket engines is much higher and the flame experiences a higher amount of strain. Therefore, the Damköhler number might take a small value and finite rate chemistry must be taken into account.

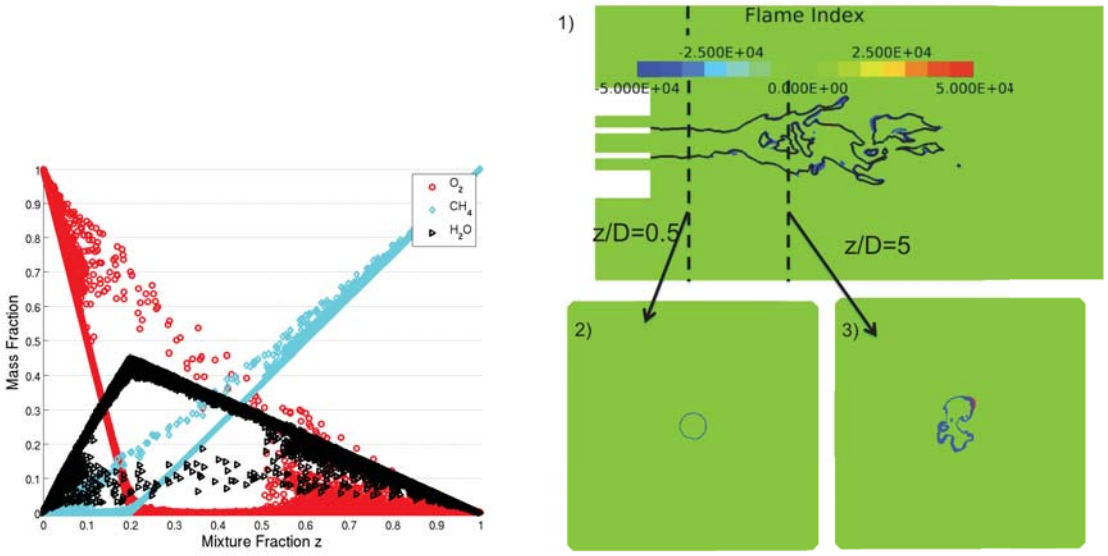

(a) (b)

Figure 8. Flame regime: (a) species versus mixture fraction scatter plot. (b) flame index Γ_f:1) plane z=0, 2) plane x=0.5D_{CH4}, 3) plane x=5D_{CH4}

It is also interesting to analyze the effect of the models defined in sections II.D and II.C on the LES temperature field. Figure 9 presents two temperature scatter plots corresponding to the two subgrid closures LAM and MAX. The points are also colored by the local oxidizer strain rate s as defined by Balakrishnan et al.[45] The cloud is compared with the simplified Burke-Schumann flame structure assuming infinitely fast chemistry and calorically perfect gas. The maximal temperature is chosen equal to the adiabatic temperature predicted by GRI-Mech 3.0 at the stoichiometry (cf. table 1). For the two cases, the evolution of the temperature is close to the Burke-Schumann solution and the maximal temperature is correctly predicted which validates the modified 1-step mechanism WD1ox. The flame obtained with the laminar chemistry, however, exhibits lots of extinctions which look unphysical, since they were not reported by the experiment. Moreover, by computing laminar Oxygen/CH4 counterflow flames, Pons et al.[46] showed that the extinction strain rate at $P = 5.6$ MPa was $s_{ext} = 10^6$ s^{-1}. Figure 10 illustrates how MAX fixes this problem. The subgrid methane reaction rate contours are plotted in color. The black contours correspond to values of the filtered reaction rate greater than 10^4 kg/m^3/s. The subgrid reaction rate is several order of magnitude lower than the LES reaction rate but it is mainly observed on the periphery of the flame in the zones where the turbulence start to strongly wrinkle the flame. The laminar chemistry closure fails to predict combustion at these locations and yields to spurious partially premixed zones which can not be correctly lighted up whereas MAX allows ignition and maintains a strict diffusion flame regime.

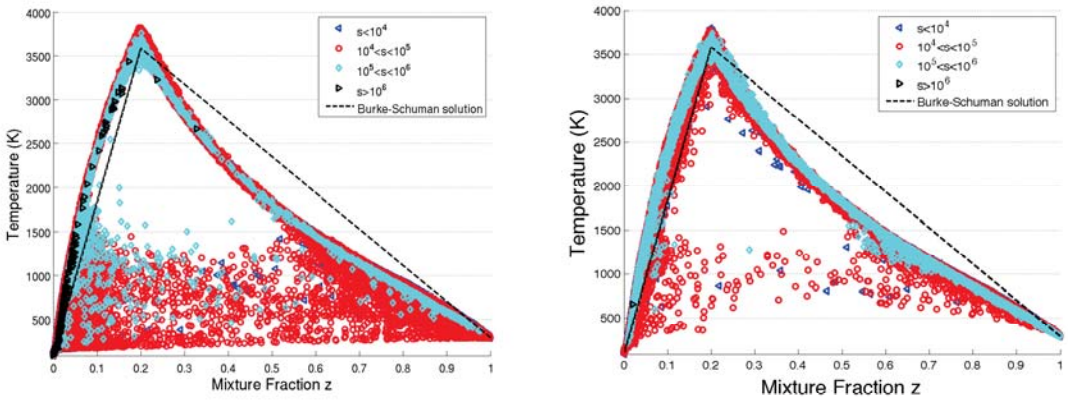

(a) (b)

Figure 9. Temperature versus mixture fraction scatter plot colored by the strain rate (/s): (a) Laminar chemistry LAM, (b) Subgrid closure MAX

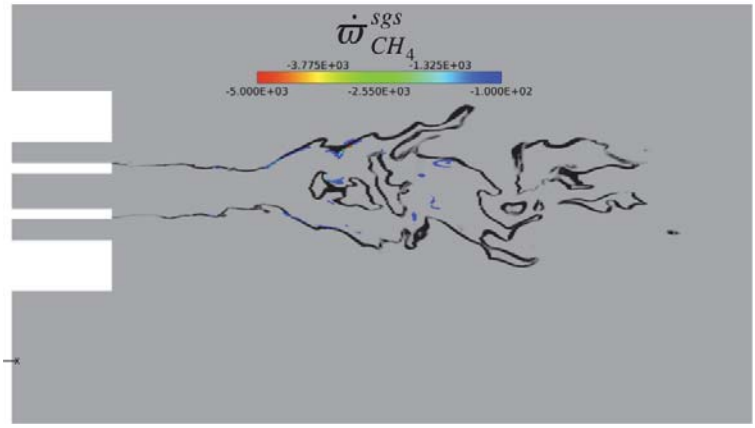

Figure 10. Methane reaction rate instantaneous field: colored contours correspond to the subgrid reaction rate $\dot{\omega}^{sgs}_{CH4}$ and black contours correspond to the filter reaction rate $|\overline{\dot{\omega}}_{CH4}| > 10^4$ kg/m^3/s.

IV.C. Real gas effects

The fluid properties variations across the flame are shown in Fig. 11. First Fig. 11a,b present the radial variations of temperature, density and species mass fraction x/D=0.5. D=0.01 m is the methane outer diameter. The density is divided by 100 between the dense oxygen and the flame. It generates very sharp density gradients in the shear layer ($0.18 < r/D < 0.3$) where both mixing and combustion occur. Then Fig. 11c shows the compressibility factor $Z = PV/RT$. This parameter measures the departure of the fluid from the ideal gas assumption. In the methane stream and in the far field ($r/D > 0.6$), Z remains close to 1 while in the oxygen core it is close to 0.2. In this zone, density predicted by the Peng Robinson equation of state is greater than 1000 Kg/m^3 while the perfect gas equation of state would provide a density around 230 Kg/m^3. Therefore, even if the perfect gas assumption might be reasonable in most of the computational domain, applying this equation of state for this case would actually entail important discrepancies on the flame expansion. This conclusion is enforced by Figs. 11d,e,f which plot the radial variation of the kinematic viscosity and the Prandtl, Lewis and Schmidt numbers. The kinematic viscosity strongly increases in the flame. The Prandtl number increases by a factor of 4 in the the LOX side of the flame to Fuel side while the Lewis number and the Schmidt numbers increases by a factor of 100. As observed by Oefelein[13] for the LOX/H2 flame, the comparison of these three numbers shows that the mass diffusion is the slowest transport phenomenon in the liquid oxygen and is rate limiting for the combustion on this side of the flame.

V. Conclusion

This paper has highlighted the results obtained in the large eddy simulation of transcritical liquid oxygen/supercritical methane flame. The solver uses a hybrid upwind central scheme to capture the large density gradients in the transcritical flow as well as the turbulence created by the shear layers and the break down of the central jet. The thermodynamics of the liquid oxygen is modeled with the Peng-Robinson cubic equation of state, which provides a good compromise between cost and accuracy for Large-Eddy Simulations. Finite-rate chemistry is modeled using a one step CH4/air which was modified to provide realistic temperatures into the CH4/O2 flame. Then the filtered reaction rate for each species is closed by correcting the resolved reaction rate with a subgrid turbulent contribution. Two simple forms of this closure have been tested. The simulation shows a good qualitative agreement with the experiment. The two combustion models achieve to stabilize the flame through the recirculation zone in the vicinity of the tip wall but the model LAM exhibits local extinctions while the second model MAX prevents them. This simple LES combustion model is a first step towards more accurate finite rate approaches able to handle a wide range of combustion regimes. Our next objective is to apply a LEM closure to this case with the same mechanism to provide a better description of the flame/turbulence interaction. A complete closure using both LEM and detailed chemistry remains too expensive to simulate real gas combustion in complex geometries. We are therefore investigating the artificial network methodology to speed up the chemistry kinetics calculation and circumvent this issue.

Acknowledgments

This research was supported by the Air Force Research Laboratory (AFRL) and Pratt & Whitney Rocketdyne. The computational resources at the DoD Supercomputing Resource Center (DSRC) and the US Army Engineering Research and Development Center (ERDC) were provided under a DOD HPC Grand Challenge Project.

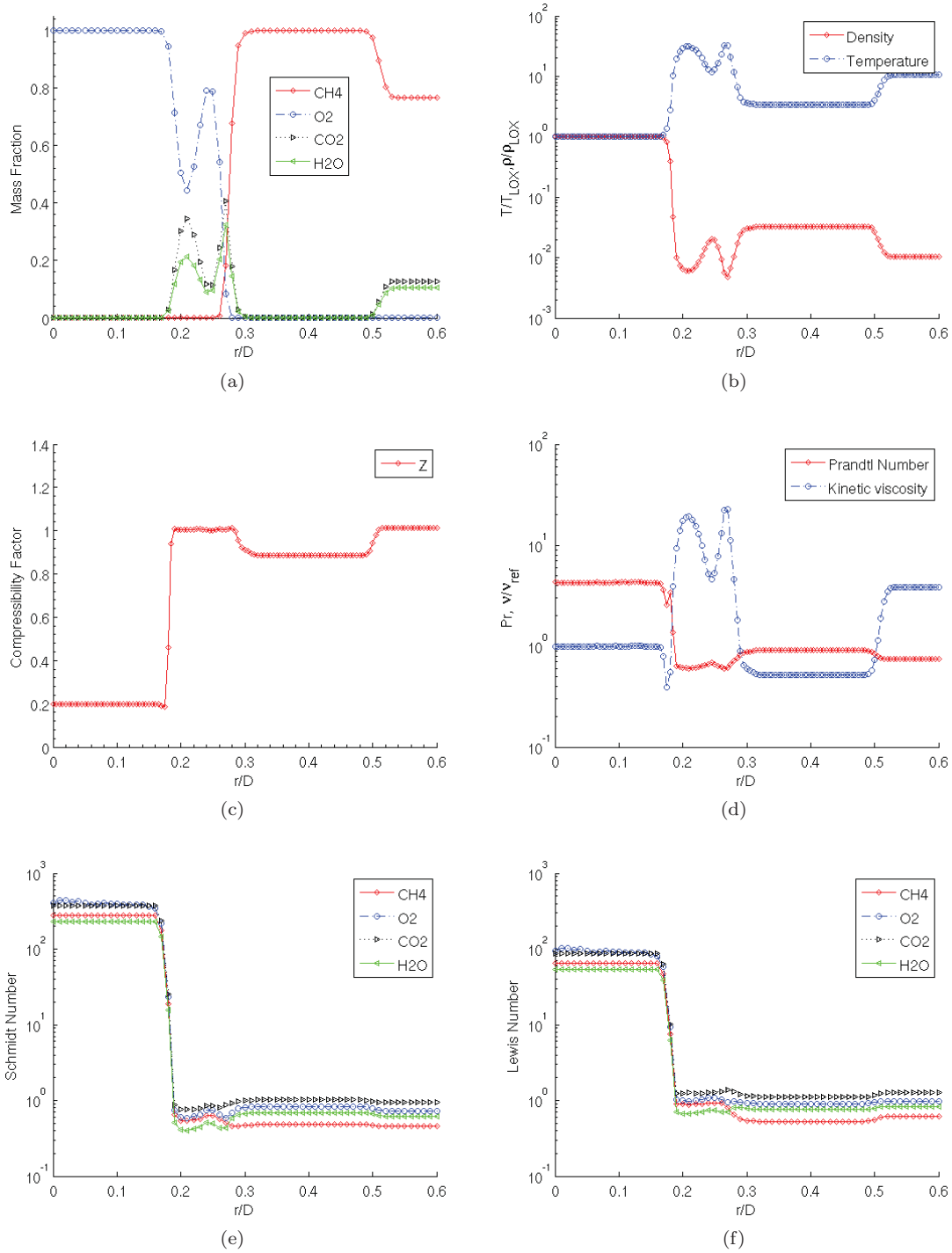

Figure 11. Radial variation of species mass fraction, temperature, density, compressibility factor, kinetic viscosity and Prantdlt, Schmidt and Lewis numbers at an axial location x/D=0.5 (D=0.01 m is the methane outer diameter)

References

[1]Poling, B. E., Prausnitz, J. M., and O'Connell, J. P., *The properties of gases and liquids*, McGraw-Hill, 5th ed., 2001.

[2]Bellan, J., "Supercritical (and subcritical) fluid behavir and modeling: drops, streams, shear and mixing layers, jets and sprays," *Progress in Energy and Combustion Science*, Vol. 26, 2000, pp. 329–366.

[3]Bellan, J., "Theory, Modeling and Analysis of Turbulent Supercritical Mixing," *Combustion Science and Technology*, Vol. 178, 2006, pp. 253–281.

[4]Oefelein, J. C., "LES of Supercritical LOX-H2 Injection and Combustion in a Shear Coaxial Uni-Element Rocket," *41st Aerospace Sciences Meeting and Exhibit*, No. AIAA 2003-0479, Reno, NV, January 2003.

[5]Prausnitz, J. M., Lichtenthaler, R., and de Azevedo, E., *Molecular thermodynamics for fluid-phase equilibrium*, 1986.

[6]Candel, S., Juniper, M., Singla, G., Scouflaire, P., and Rolon, C., "Structure and dynamics of cryogenic flames at supercritical pressure," *Combustion science and technology*, Vol. 178, No. 1-3, 2006, pp. 161–192.

[7]Oschwald, M., Smith, J., Branam, R., Hussong, J., Schik, A., Chehroudi, B., and Talley, D., "Injection of fluids into supercritical environments," *Combustion science and technology*, Vol. 178, No. 1-3, 2006, pp. 49–100.

[8]Mayer, W. and Tamura, H., "Propellant injection in a liquid oxygen/gaseous hydrogen rocket engine," *Journal of Propulsion and Power*, Vol. 12, No. 6, 1996, pp. 1137–1147.

[9]Yang, B., Cuoco, F., and Oschwald, M., "Atomization and Flames in LOX/H2 and LOX/CH4-Spray Combustion," *Journal of Propulsion and Power*, Vol. 23, 2007, pp. 763–771.

[10]Harstad, K. G., Miller, R. S., and Bellan, J., "Efficient High-Pressure State Equations," *American Institute of Chemical Engineers Journal*, Vol. 43, No. 6, 1997, pp. 1605–1610.

[11]Oefelein, J. and Yang, V., "Modeling high-pressure mixing and combustion processes in liquid rocket engines," *J. Propulsion & power*, Vol. 14, No. 5, 1998.

[12]Zong, N. and Yang, V., "Cryogenic fluid jets and mixing layers in transcritical and supercritical environments," *Combustion science and technology*, Vol. 178, No. 1-3, 2006, pp. 193–227.

[13]Oefelein, J., "Mixing and combustion of cryogenic oxygen-hydrogen shear-coaxial jet flames at supercritical pressure," *Combustion science and technology*, Vol. 178, No. 1-3, 2006, pp. 229–252.

[14]Singla, G., Scouflaire, P., Rolon, C., and Candel, S., "Transcritical oxygen/transcritical or supercritical methane combustion," *Proceedings of the Combustion Institute*, Vol. 30, 2005, pp. 2921–2928.

[15]Masquelet, M. and Menon, S., "Large-Eddy Simulation of flame-turbulence interaction in a shear coaxial injection," *J. Prop. Power* , Vol. 26-5, 2010, pp. 924–935.

[16]Ó Conaire, M., Curran, H., Simmie, J., Pitz, W., and Westbrook, C., "A comprehensive modeling study of hydrogen oxidation," *International journal of chemical kinetics*, Vol. 36, No. 11, 2004, pp. 603–622.

[17]Smith, G. P., Golden, D. M., Frenklach, M., Moriarty, N. W., Eiteneer, B., Goldenberg, M., Bowman, C. T., Hanson, R. K., Song, S., Gardiner, William C. Jr.and Lissianski, V. V., and Qin, Z., "GRI-MECH 3.0, `http://www.me.berkeley.edu/gri_mech`," .

[18]Huo, H. and Yang, V., "Supercritical LOX/Methane Combustion of a Shear Coaxial Injector," *49th AIAA Aerospace Sciences Meeting including the New Horizons Forum and Aerospace Exposition*, Orlando, Florida, 2011.

[19]Patel, N. and Menon, S., "Simulation of spray-turbulence-flame interactions in a lean direct injection combustor," *Combustion and Flame*, Vol. 153, No. 1-2, 2008, pp. 228–257.

[20]Cutrone, L., De Palma, P., Pascazio, G., and Napolitano, M., "A RANS flamelet-progress-variable method for computing reacting flows of real-gas mixture," *Computers & Fluids*, Vol. 39, 2010, pp. 485–498.

[21]Schmitt, T., Méry, Y., Boileau, M., and Candel, S., "Large-Eddy Simulation of oxygen/methane flames under transcritical conditions," *Proceedings of the Combustion Institute*, Vol. 33, 2011, pp. 1383–1390.

[22]Erlebacher, G., Hussaini, M. Y., Speziale, C. G., and Zang, T. A., "Toward the Large-Eddy Simulation of Compressible Turbulent Flows," *Journal of Fluid Mechanics*, Vol. 238, 1992, pp. 155–185.

[23]Fureby, C. and Møller, S. I., "Large eddy simulations of reacting flows applied to bluff body stabilized flames," *AIAA Journal* , Vol. 33, No. 12, 1995, pp. 2339.

[24]Veynante, D., Trouvé, A., Bray, K. N. C., and Mantel, T., "Gradient and counter-gradient transport in turbulent premixed flames," *Rapport du Centre de Recherche sur la Combustion Turbulente*, edited by T. J. Poinsot, T. Baritaud, and M. Baum, Technip, Rueil Malmaison, 1996, pp. 183–200.

[25]Ribert, G., Zong, N., Yang, V., Pons, L., Darabiha, N., and Candel, S., "Counterflow Diffusion Flames of General Fluids: Oxygen/Hydrogen Mixtures," *Combustion and Flame*, Vol. 154, 2008, pp. 319–330.

[26]Menon, S. and Patel, N., "Subgrid Modeling for Simulation of Spray Combustion in Large-Scale Combustors," *AIAA Journal*, Vol. 44, No. 4, April 2006, pp. 709–723.

[27]Chakravarthy, V. K. and Menon, S., "Subgrid Modeling of Premixed Flames in the Flamelet Regime," *Flow, Turbulence and Combustion*, Vol. 65, 2001.

[28]Hirschfelder, J., Curtis, C., and Bird, B., *Molecular Theory of Gases and Liquids*, John Wiley & Sons, 1954th ed., 1954.

[29]Chung, S. H. and Law, C. K., "An invariant derivation of flame stretch," *Combust. Flame* , Vol. 55, 1984, pp. 123–125.

[30]Fuller, E. N., Paul D. Schettler, J., and Giddings, C., "NEW METHOD FOR PREDICTION OF BINARY GAS-PHASE DIFFUSION COEFFICIENTS," *Ind. Eng. Chem.*, Vol. 58, 1966, pp. 18–27.

[31]Westbrook, C. K., Adamczyk, A. A., and Lavoie, G. A., "A numerical study of laminar flame wall quenching." *Combustion and Flame*, Vol. 40, 1981, pp. 81–99.

[32]Poinsot, T. and Veynante, D., *Theoretical and Numerical Combustion*, R.T. Edwards, 2nd edition, 2005.

[33]Spalding, D. B., "Mixing and chemical reaction in steady confined turbulent flames," *13th Symp. (Int.) on Combustion*, The Combustion Institute, Pittsburgh, 1971, pp. 649–657.

[34]Spalding, D. B., "Development of the Eddy-Break-Up model of turbulent combustion," *16th Symp. (Int.) on Combustion*, The Combustion Institute, 1976, pp. 1657–1663.

[35]Magnussen, B. F. and Hjertager, B. H., "On mathematical modeling of turbulent combustion," *16th Symp. (Int.) on Combustion*, The Combustion Institute, Pittsburgh, 1976, pp. 719–727.

[36]Magnussen, B. F., "On the Structure of Turbulence and a Generalized Eddy Dissipation Concept for Chemical Reaction in Turbulent Flow," *Nineteenth AIAA Aerospace Meeting*, Saint Louis, 1981.

[37]Magnussen, B. F., "Modeling of Pollutant Formation in Gas Turbine Combustors Based on the Eddy Dissipation Concept." *Eighteenth International Congress on Combustion Engines*, International Council on Combustion Engines, Tianjin, China., 1989.

[38]Singla, G., Scouflaire, P., Rolon, C., and Candel, S., "Planar laser-induced fluorescence of OH in high-pressure cryogenic LOx/GH2 jet flames," *Combustion And Flame*, Vol. 144, 2006, pp. 151–169.

[39]Masquelet, M., *Simulations of a Sub-scale Liquid Rocket Engine: Transient Heat Transfer in a Real Gas Environment*, Master's thesis, Georgia Institute of Technology, December 2006.

[40]Masquelet, M., Menon, S., Jin, Y., and Friedrich, R., "Simulation of unsteady combustion in a LOX-GH_2 fueled rocket engine," *Aerospace Science and Technology*, Vol. 13, No. 8, December 2009, pp. 466–474.

[41]Génin, F., Fryxell, B., and Menon, S., "Hybrid Large-Eddy Simulation of Detonation in Reactive Mixtures," *Proceedings of the 20th International Conference on Detonations, Explosions and Shock Waves*, Montreal, Canada, August 2005.

[42]Génin, F. and Menon, S., "Studies of Shock/Turbulent Shear Layer Interaction Using Large-Eddy Simulation," *Computers and Fluids*, Vol. 39, 2008, pp. 800–819.

[43]Toro, E., Spruce, M., and Speares, W., "Restauration of the Contact Surface in the HLL Riemann Solver," *Shock Waves*, Vol. 4, 1994, pp. 25–34.

[44]Yamashita, H., Shimada, M., and Takeno, T., "A numerical study on flame stability at the transition point of jet diffusion flame," *26th Symp. (Int.) on Combustion*, The Combustion Institute, Pittsburgh, 1996, pp. 27 – 34.

[45]Balakrishnan, G., Trevino, C., and Mauss, F., "The Asymptotic Structure of Hydrogen-Air Diffusion Flames," *Combust. Flame* , Vol. 91, 1992, pp. 246–256.

[46]Pons, L., Darabiha, N., and Candel, S., "Pressure effects on nonpremixed strained flames," *Combustion and Flame*, Vol. 152, No. 1, 2008, pp. 218–229.